



Collective spin 1 singlet phase in high-pressure oxygen

Yanier Crespo^a, Michele Fabrizio^b, Sandro Scandolo^a, and Erio Tosatti^{a,b,1}

Author Affiliations

Edited by David Vanderbilt, Rutgers, The State University of New Jersey, Piscataway, NJ, and approved June 13, 2014 (received for review March 11, 2014)

Abstract Full Text Authors & Info Figures Metrics Related Content

Significance

Among the elemental diatomic molecules, O_2 is the only one carrying a spin 1 magnetic moment. In the high pressure phases of oxygen the magnetic moment conspires with intermolecular forces to generate a rich phase diagram. Whereas, up to 80,000 atmospheres the moment persists, at pressures between 80,000 and 200,000 atmospheres, molecular magnetism apparently disappears, however with a number of unexplained vibrational and optical anomalies. Through a fully quantum treatment of the electronic states of the dense crystalline state we find that in this pressure range oxygen still retains a spin moment in an unconventional and rare state of matter dominated by the quantum fluctuations. This state, a special case of so-called spin liquids, explains most of the observed anomalies.

Collective spin 1 singlet phase in high pressure oxygen

Y. Crespo,¹ M. Fabrizio,² S. Scandolo,¹ and E. Tosatti^{1,2}

¹The Abdus Salam ICTP, Strada Costiera 11, I-34151 Trieste, Italy

²International School for Advanced Studies (SISSA),
and CNR-IOM Democritos, Via Bonomea 265, I-34136 Trieste, Italy

This work has just been published in PNAS, 111, 10427 (2014): Oxygen, one of the most common and important elements in nature, has an exceedingly well explored phase diagram under pressure, up and beyond 100 GPa. At low temperatures, the low pressures antiferromagnetic phases below 8 GPa where O_2 molecules have spin $S=1$ are followed by the broad apparently nonmagnetic ϵ phase from about 8 to 96 GPa. In this phase which is our focus molecules group structurally together to form quartets while switching, as believed by most, to spin $S=0$. Here we present theoretical results strongly connecting with existing vibrational and optical evidence, showing that this is true only above 20 GPa, whereas the $S=1$ molecular state survives up to at about 20 GPa. The ϵ phase thus breaks up into two: a spinless ϵ_0 (20–96 GPa), and another ϵ_1 (8–20 GPa) where the molecules have $S=1$ but possess only short range antiferromagnetic correlations. A local spin liquid-like singlet ground state akin to some earlier proposals and whose optical signature we identify in existing data, is proposed for this phase. Our proposed phase diagram thus has a first order phase transition just above 20 GPa, extending at finite temperature and most likely terminating into a crossover with a critical point near 30 GPa and 200 K.

PACS numbers:

Keywords: epsilon oxygen | high pressure | phase transition | spin singlets

I. INTRODUCTION

Molecular systems display at high pressure a horn of plenty of intriguing phases. That is especially true of molecular oxygen, whose diatomic molecule survives unbroken up to at least 133 GPa¹, and where the original spin $S=1$ of the gas phase plays an important role. In the phase diagram of O_2 (Fig.1) we focus on the wide ϵ - O_2 phase between 8 and 96 GPa, a phase which has long intrigued the community². Unlike the two bordering phases, δ - O_2 an antiferromagnetic (AF) $S=1$ cor-

related insulator at lower pressure, and ζ - O_2 a regular and superconducting nonmagnetic (NM) metal at higher pressure, ϵ - O_2 is an insulator of more complex nature. Structurally, high-pressure X-ray diffraction^{3,4} revealed in the last decade that at the $\delta - \epsilon$ transition at $P \approx 8$ GPa the close-packed O_2 planes undergo a large distortion giving rise to molecular O_8 “quartets”, (inset in Fig.1). Spin-polarized neutron diffraction showed that simultaneously there is a collapse of long-range AF Néel order at the $\delta - \epsilon$ transition⁵. That observation unfortunately did not provide conclusive information about the

This Issue



July 22, 2014
vol. 111 no. 29
Masthead (PDF)
Table of Contents

PREV ARTICLE NEXT ARTICLE

Don't Miss

PNAS announces its participation in SocialCite, a new tool that improves the citation network by allowing you to provide feedback about the validity and quality of citations.

Article Tools

Article Alerts
Export Citation
Save for Later
Request Permission

Share

nature of the ground state in ϵ -O₂ and in particular about any further role played in ϵ -O₂ by the spin of individual molecules if any. It has been tempting to imagine that the O₂ molecular magnetic state could simply collapse from $S=1$ to $S=0$ at the $\delta - \epsilon$ transition. In support of this idea it can be noted that the metallic state band structure of a hypothetical undistorted nonmagnetic O₂⁶ is prone to turn spontaneously insulating through a Peierls type distortion, for example dimerizing^{7,8}, or tetramerizing⁹ the molecules. Further density functional theory (DFT) calculations strengthened that picture, showing the quartet distorted geometry¹⁰ drives the undistorted metal to a band insulator. Moreover, DFT calculations showed that this state exhibits O₂ vibrations whose frequency and pressure evolution are, between 20 and 96 GPa, in good agreement with infrared (IR) and Raman data¹¹ (see Fig.3(a)).

An alternative, much more speculative picture insisting instead on a correlated state where O₂ retains its $S=1$ gas phase spin, and where the quartet of AF coupled sites yields a singlet ground state as the basic O₈ block of ϵ -O₂,¹² provided no such successful predictions and had limited following so far – see however Ref.13.

Let us provide first some background before embarking in theoretical calculations. Several experimental authors^{7,14–17} had noted that the behaviour of O₂ in the 8-20 GPa pressure range is in many ways anomalous compared with that above 20 GPa¹⁸. Focusing on O₂ vibrations, the good agreement found by Pham *et al.*¹¹ between the band insulator calculations and the measured IR and Raman frequencies (Fig.3(a)) is limited to above $P > 20$ GPa. Below this pressure, the IR mode reverts non-monotonically upwards approaching the high frequency Raman mode at the δ -O₂ phase boundary of 8 GPa, rather than dropping steadily as predicted by the band insulator. Subtly, but not less significantly, the O₂ Raman data (Fig.3(a)) show that 20 GPa marks a delicate but definite breaking point with a lower rate of decrease of the mode frequency with decreasing pressure. Both IR and Raman elements hint at a possible switch of individual O₂ molecules from $S = 0$ to $S = 1$ upon decreasing pressure near 20 GPa. In particular, the frequency gap between the IR mode, where nearest neighbour O₂ vibrate out of phase, and the Raman mode where they vibrate in phase (see insets in Fig.3(a)) is proportional to the IR effective charge, connected with electron current “pumping” between an instantaneously extended molecule (which attracts electrons) and a neighboring compressed one (which expels them) in the IR mode. This electron current is absent in the Raman mode, where neighboring molecules vibrate in phase. If the molecules have spin and correlations are strong, the electron hopping is reduced and the current magnitude, proportional to the IR effective charge, must drop compared to the nonmagnetic band state. Thus the onset of molecular spin upon decreasing pressure should be accompanied by a collapse of the IR intensity and of the IR -Raman splitting, as is indeed observed (see In-

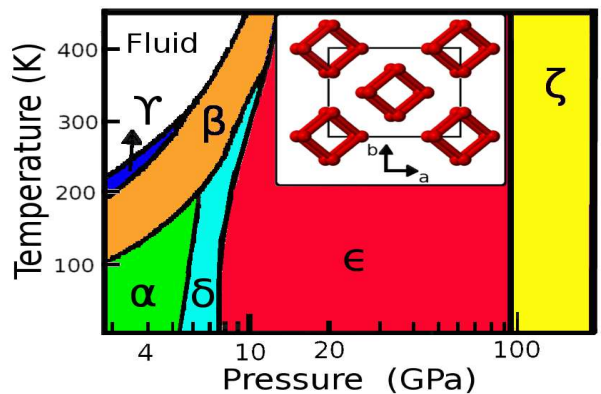


Figure 1: (Color online) Currently accepted phase diagram of oxygen (adapted from Ref.²). The inset shows the unit cell of ϵ -O₂^{3,4}

set in Fig.5). With this background, experimental facts suggest dividing the vast ϵ -O₂ phase into two. A higher pressure phase between 20 and 96 GPa, which we may call ϵ_0 -O₂, where there is no molecular spin and whose physics including lattice vibrations is well described as a band insulator whose gap is due to the Peierls-like quartet distortion, and a lower pressure phase between 8 and 20 GPa which we shall call ϵ_1 -O₂ where that picture fails, and molecular spin probably resurrects signaling that strong correlations coexist within the quartet distortion of the molecules. The long range Néel order typical of the lower pressure undistorted phases is absent here, suggesting that it might be replaced by some kind of correlated singlet state such as that of Ref.12. However, strong and verifiable predictions about the same measured vibrational and optical that are well described by the band insulator in ϵ_0 -O₂ have not been advanced for this type of state.

Our work has the following aims: (i) Provide first principles quantitative calculations of electronic and vibrational properties of same quality for both ϵ_0 -O₂ and ϵ_1 -O₂, including Raman and IR vibrational frequencies and intensities that could be compared with experiment in both regimes. The approach should allow, even if at the approximate mean field level, for the presence of molecular spin whenever that should lower the total enthalpy; (ii) Describe the nature, stability, and optical properties of the resulting model $S=1$ collective singlet state description of ϵ_1 -O₂, extending that in literature^{12,13}, particularly including quantum fluctuations and ; (iii) Predict the new phase diagram displaying a first order $\epsilon_1 - \epsilon_0$ low temperature phase transition near 20 GPa, and a novel phase line predicting at high temperature a new critical point roughly at 30 GPa and 200 K inside the broad ϵ -O₂ phase.

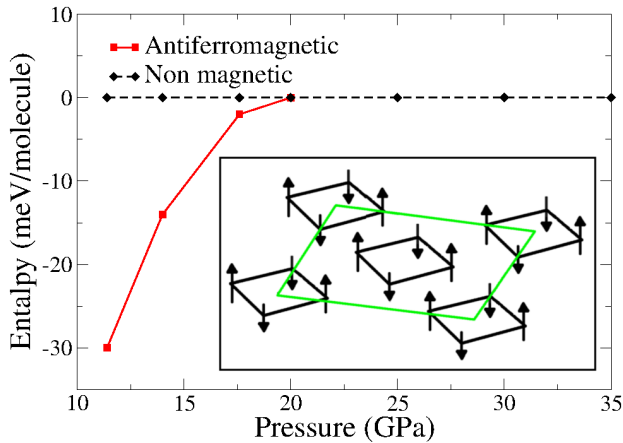


Figure 2: Enthalpy difference calculated by DFT+ U between non-magnetic and antiferromagnetic states in ϵ -O₂. Inset: antiferromagnetic configuration inside the O₈ “quartets”.

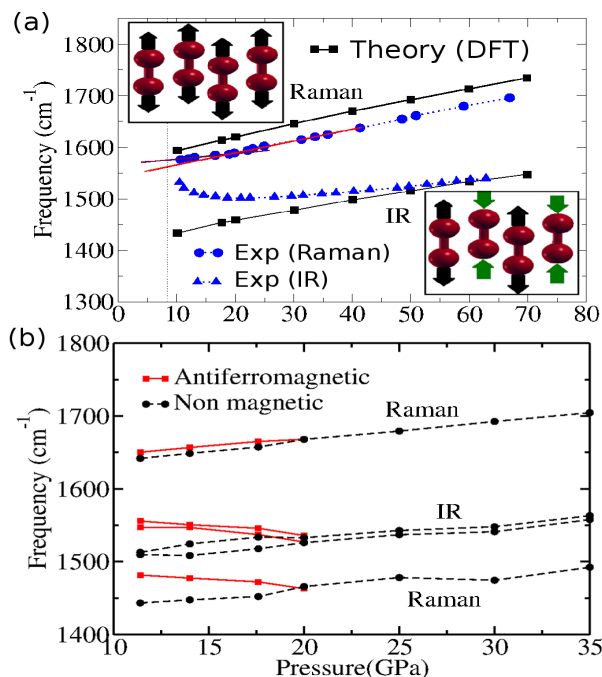


Figure 3: (Color online) Vibrational frequencies of the O₂ stretching modes as a function of pressure. (a) Solid line with squares: calculated Raman and IR modes from Ref.¹¹. Dashed line with circles: Raman mode data from Ref.¹⁶. Dashed line with triangles: IR mode data from Ref.⁷. Displacement patterns for the IR and Raman modes are shown in the lower right and upper left insets, respectively. (b) Calculated Raman and IR modes for the non-magnetic and the antiferromagnetic configurations (this work).

II. FIRST PRINCIPLES CALCULATIONS AND RESULTS

Our starting point is a density-functional theory (DFT) electronic structure calculation with full struc-

tural optimization for the whole ϵ -O₂ pressure range. We employed spin-polarized, self-interaction corrected calculations (DFT+ U)^{19–21} as implemented in Quantum-Espresso²². By allowing for static magnetic polarization we permit the possible presence of molecular spin to emerge – of course at the price of assuming it to exist in static and thus symmetry-breaking form. The GGA exchange-correlation functional was employed in the version of Perdew, Burke and Ernzerhof²³, and DFT+ U calculations were carried out in the simplified version of Dudarev *et al.*²⁴ as implemented in the Quantum-Espresso code²⁵. The inclusion of a Hubbard U for oxygen p-states is called for to provide cancellation of self-interactions still present in simple generalized gradient approximation (GGA) DFT. Whereas for the uncorrected choice $U=0$ the calculated band gap is unrealistically small and spin polarization does not arise,^{10,11} calculations in a reasonable range of values of the parameter U (0.8, 1.0, 1.5 and 2.0 eV) yield antiferromagnetism below 17.6, 20.0, 25.0 and 30.0 GPa respectively. We selected $U=1.0$ eV, as the value yielding the transition pressure that fits more reasonably the experimental findings to be described below in the vibrational spectra.^{7,14,16} Their frequency and intensity behaviour does not change with the value of U . We note that this method to reduce self-interactions is convenient but by no means unique, and other possibilities such as hybrid functional approximations could have been adopted. A $4 \times 4 \times 4$ Monkhorst-Pack k-point mesh²⁶ Brillouin zone sampling was used throughout. The crystal structure (C2/m) and the initial atomic positions were taken from the experimental data⁴. Lattice and internal parameters were then fully optimized at different pressures until forces were smaller than 10^{-5} a.u. The vibrational spectra were calculated using the *fropho* code that calculates phonons based on the Parlinski-Li-Kawazoe method²⁷. Infrared intensities were calculated by density functional perturbation theory²⁸ by single-point DFT calculations with the fully DFT+ U relaxed crystal structures.

The optimized structure has O₂ molecules forming quartets in each plane, quite close to the experimental ones⁴. A clear AF state prevails below 20 GPa, as shown by the enthalpy difference of Fig.2 between the NM and the AF state, where molecules are simultaneously quartet distorted and antiferromagnetically spin polarized. As anticipated, the predicted low pressure resurgence of molecular spin comes with an unrealistic AF static long range order which is absent in experiment⁵. How this artificial mean-field symmetry breaking can be removed by quantum fluctuations will be described later. Ignoring that for the moment, and assuming the mean-field to yield as usual a reasonable total energy, we can exploit our first principles calculations to obtain a prediction for the change of other properties brought about by the instantaneous presence of molecular spin. We calculated, with the DFT+ U approach, the vibrational spectra of both the nonmagnetic and magnetic states of ϵ -O₂. As is shown in Fig.3(b) the onset of spin breaks the mono-

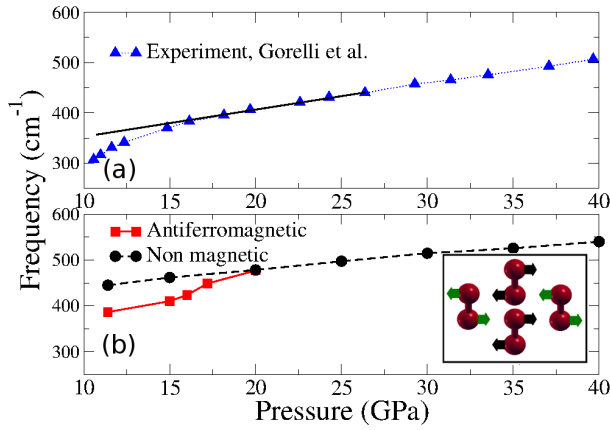


Figure 4: Frequency of the far-IR vibrational mode as a function of pressure. (a) Data from Ref.⁷ (b) Calculations using the non magnetic and the antiferromagnetic configurations. Inset: calculated displacement pattern of the far-IR mode.

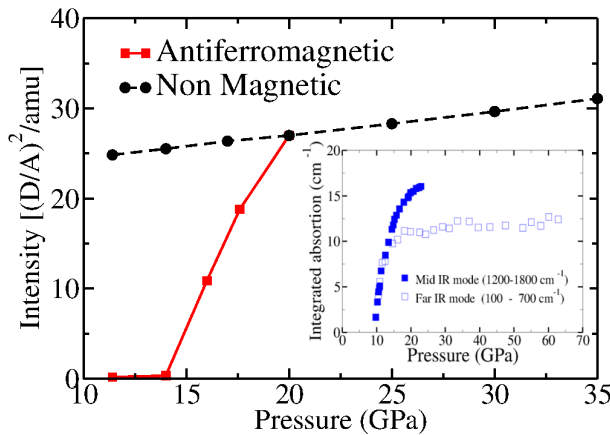


Figure 5: (Color online) Calculated Intensities for mid-IR modes (1500-1600 cm^{-1}) of both non-magnetic and antiferromagnetic configurations (this work). Inset: solid squares, measured IR intensities of the mid-IR mode (1200-1800 cm^{-1}); open squares, far IR mode (200-600 cm^{-1}) intensities from Ref.⁷

tonic drop of both Raman and IR mode frequencies with decreasing pressure, that was predicted for the non-magnetic state by previous calculations¹¹ but which did not agree with experiment below 20 GPa. Direct comparison of Fig.3(b) with Fig.3(a) shows now a better agreement, confirming that both the non-monotonic rise of the IR mode and the slight stiffening of the Raman mode are spin-related. Many other phonon modes are also influenced by the onset of spin.

In Fig.4 our calculated evolution of the main far infrared vibrational mode (see Fig.4 (b)), is shown to drop below 20 GPa in agreement with experimental data (see Fig.4 (a)). This evolution of both high and low frequency IR modes upon lowering pressure below 20 GPa goes together with a corresponding change – in fact a decrease – of the mode effective charge. Fig.5 shows that the dra-

matic drop of the IR intensity observed in this regime (see Inset in Fig.5), so far unexplained, is now well accounted for by the onset of molecular spin.

We already hinted at the main physical reasons why spin causes all these changes in the vibrational spectrum. The first element is that spin arises in connection with strong electron correlations, which characterize all lower pressure phases including $\delta\text{-O}_2$. In the strongly correlated state, O_2 molecules reduce their mutual electron hopping, and tend to revert toward their gas phase state, which has spin 1, with shorter bond length and about 71 cm^{-1} higher vibrational frequency²⁹. That explains why the highest (intramolecular) Raman mode reduces its softening rate below 20 GPa (see Fig.3). The reduced IR effective charge, and the shrinking of the frequency gap between the out-of-phase IR and the in-phase Raman modes as calculated and observed implies a reduced inter-molecular electron hopping in the AF correlated state.

For our subsequent understanding of the magnetic state below 20 GPa it is also important to estimate the effective Heisenberg exchange couplings among O_2 molecules. Calling J_1, J_2, J_3 and J_4 the exchange values between the first, second, third and fourth neighbors (see Fig.6) we carried out constrained spin polarized DFT+ U calculations, based on the experimental structure at $P = 11.4 \text{ GPa}$ ³ and a variety of six different AF configurations. Fitting these results we obtained $J_1 = 170.0 \pm 30 \text{ meV}$, $J_2 = 35.5 \pm 2 \text{ meV}$, $J_3 = 10.5 \pm 2 \text{ meV}$, $J_4 = 14.4 \pm 4 \text{ meV}$. On account of the mean-field nature of the DFT calculations, these values are probably somewhat larger values than real, and should be considered upper bounds.

III. LATTICE SINGLET MODEL AND QUANTUM FLUCTUATIONS OF $S=1$ SPINS

The previous section showed that the resurgence of molecular spin below 20 GPa could simultaneously explain several observed O_2 vibrational anomalies. However the mean-field long range AF order obtained by DFT disagreed with the lack of long range spin order found experimentally⁵. A state where molecular spins are present without $T = 0$ long-range order would constitute a kind of spin 1 liquid. In this section we discuss, extending the picture earlier proposed by Gomony and Loktev¹² and more recently pursued by Bartolomei *et al.*¹³ consisting of an overall singlet state of an isolated quartet of $S = 1$ molecules.

The quantum mechanical competition between AF long range order and an overall singlet state must be pursued in the whole $\epsilon_1\text{-O}_2$ lattice. For that purpose we simplify the system as a 2D square lattice model made of plaquettes (quartets) of $S = 1$ Heisenberg sites. Each site, representing an O_2 molecule, is AF coupled to nearest neighbours within the same plaquette by AF exchange couplings $J_1 > 0$, and to nearest neighbours in the next plaquettes by $J_2 < J_1$, see Fig.7. Two different states compete: the Néel AF configuration, as ob-

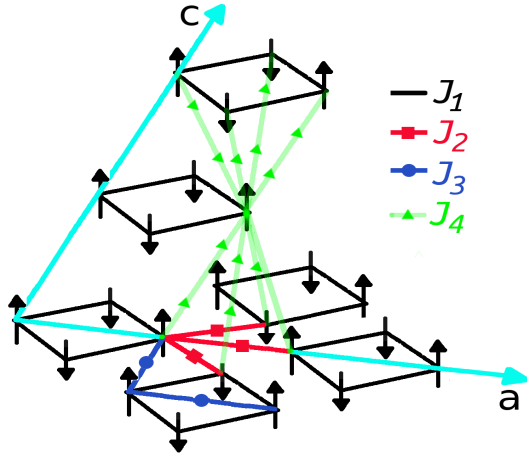


Figure 6: (Color online) Long range antiferromagnetic order and interactions between the first fourth neighbors J_1 (inside the quartet), J_2 with the two or three nearest quartets, J_3 third nearest neighbors in the plane and J_4 with molecules located in the planes above and below.

tained by DFT and which breaks spin $SU(2)$ symmetry, and a singlet, NM state that is akin to a collection of independent plaquettes, each in its singlet ground state. The singlet ground state of an isolated plaquette of energy $E_0 = -6J_1$ is obtained by coupling second neighbor sites 1 and 3 to $S_{13} = S_1 + S_3 = 2$, sites 2 and 4 to $S_{24} = S_2 + S_4 = 2$, see Fig.7, and then coupling S_{13} and S_{24} to a total singlet $S = S_{13} + S_{24} = 0$. The energy per site of an independent collection of plaquettes thus is (note that the number of plaquettes N_{\square} is one quarter the number of sites)

$$E_{\square} = -\frac{3}{2} J_1. \quad (1)$$

By comparison, the classical energy per site of the Néel AF configuration is

$$E_{\text{Neél}} = -J_1 - J_2, \quad (2)$$

Therefore, for $J_2 < J_1/2$ the non-magnetic collection of independent plaquettes will be lower in energy than the Néel configuration. If we use $J_2 \simeq 35$ meV and $J_1 \simeq 170$ meV $> 2J_2$, we may conclude that the actual ground state is a collection of independent non-magnetic plaquettes. This state is akin to that proposed in Ref.¹². We observe further that the next-nearest-neighbor exchange $J_3 > 0$ frustrates and penalizes the Néel configuration more than the non-magnetic one, leading to the energy balance within each plaquette from $E_{\square} - E_{\text{Neél}} = -J_1/2 + J_2 \rightarrow -J_1/2 + J_2 - J_3/2$. Moreover, the inter-plane exchange J_4 gives no contribution to the classical energy, since its effects cancel out as can be seen in Fig.6. Since both J_3 and J_4 are anyhow smaller than J_2 , we shall not consider them in the following analysis. The above treatment however is still crude, as it does not take into account quantum fluctuations. To evaluate

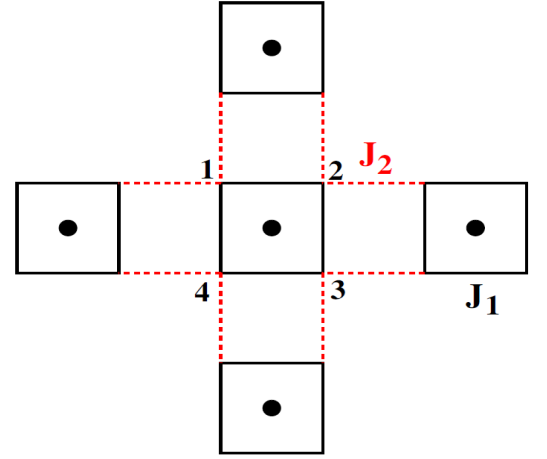


Figure 7: (Color online) Simplified two-dimensional Heisenberg model.

their impact we assess the stability of the non-magnetic state against quantum fluctuations. Elementary quantum fluctuations are built by combining into an overall singlet two separate spin fluctuations in neighboring plaquettes. The first excited state of the isolated plaquette is still obtained by $S_{13} = 2$ and $S_{24} = 2$, now coupled into a total spin $S = S_{13} + S_{24} = 1$, at energy J_1 above the ground state. Let us denote as $|\mathbb{S}\rangle$ the plaquette singlet ground state, and $|\mathbb{T}, M\rangle$ the excited triplet with $S_z = M = -1, \dots, +1$. If we consider two nearest neighboring plaquettes, identified by the positions \mathbf{R} and \mathbf{R}' , application of the exchange J_2 to the state in which both plaquettes are in the ground state

$$H_{J_2} |\mathbb{S}; \mathbf{R}\rangle |\mathbb{S}; \mathbf{R}'\rangle = -J_2 \sum_{M=-1}^{+1} (-1)^M \times |\mathbb{T}, M; \mathbf{R}\rangle |\mathbb{T}, -M; \mathbf{R}'\rangle, \quad (3)$$

excites in both plaquettes the spin-triplet configurations, with the two coupled to a singlet. This process has an amplitude $\sqrt{3} J_2$. These two excitations could move, still remaining in a full singlet configuration,

$$H_{J_2} |\mathbb{S}; \mathbf{R}\rangle |\mathbb{T}, M; \mathbf{R}'\rangle = -J_2 |\mathbb{T}, M; \mathbf{R}\rangle |\mathbb{S}; \mathbf{R}'\rangle. \quad (4)$$

They are not independent, since they gain an energy $-J_2/4$ when they are nearest neighbour. This attraction however cannot overcome the hard-core constraint, since the two triplets cannot reside on the same plaquette. The problem is thus equivalent to two hard-core bosons, each costing an energy J_1 and able to hop between nearest neighbour plaquettes with an amplitude $-J_2$. In spite of the weak nearest neighbour attraction $-J_2/4$, their lowest energy state is unbound and has energy $2J_1 - 8J_2$. The overall singlet, spin liquid state will be stable so long as this excitation gap is positive, whereas antiferromagnetism will prevail if it is zero or

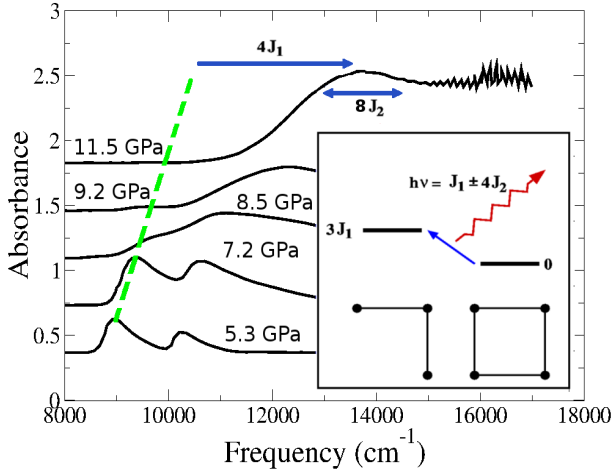


Figure 8: (Color online) Explanation of the blue shift at the $\delta \rightarrow \epsilon$ transition. Solid lines are data of the IR absorption from Ref.¹⁵, dashed green line is a linear extrapolation of the peak corresponding to ${}^3\Sigma_g^- \rightarrow {}^1\Delta_g$ process at 11.5 GPa, the blue arrow represents the blue shift of $4J_1$ with a $8J_2$ broadening represented by the double blue arrow. Inset: Initial “plaquette” and final $S = 1$ trimer state; an itinerant spin-1 excitation is emitted by spin conservation (red wavy arrow) which costs an additional energy of $h\nu \simeq 4(J_1 \pm J_2)$.

negative. Based on this result, a better estimate for the stability of the overall singlet is the condition $2J_1 \gtrsim 8J_2$, which leads to $J_2 < J_1/4$. The estimated values of the exchange couplings satisfy this inequality, confirming the stability of an overall singlet state, even once quantum fluctuations are included. The spin liquid singlet state, a lattice of plaquettes each made of four antiferromagnetically correlated $S=1$ sites, with weaker but nonzero inter-plaquette correlations, represents in conclusion our best model for ϵ_1 -O₂ below 20 GPa.

A. Infrared spectrum in the lattice singlet model

One burning question is at this point what evidence can one identify proving the existence of a nonzero molecular spin in low pressure ϵ -O₂, despite its lack of magnetic long-range order. There is in fact at least one such evidence, long published that but not interpreted yet, and it is optical. Near infrared spectroscopy across the δ - ϵ transition shows the excitation of a single O₂ molecule from its lowest energy ${}^3\Sigma_g^-$ $S=1$ configuration to the lowest $S=0$ ${}^1\Delta_g$ state. This process, forbidden by spin and parity in isolated O₂, is allowed in a lattice of molecules and shows up in high pressure optical absorption¹⁵. The peak corresponding to ${}^3\Sigma_g^- \rightarrow {}^1\Delta_g$ (and its first vibrational satellite, triggered by molecular elongation in the $S=0$ state) is clearly visible in the δ -phase, at an energy $\sim 8 - 9.000 \text{ cm}^{-1}$, a frequency comparable to that of the isolated molecule. When the ϵ -phase sets in above 8 GPa the ${}^3\Sigma_g^- \rightarrow {}^1\Delta_g$ is abruptly blue shifted to $\sim 12.400 \text{ cm}^{-1}$

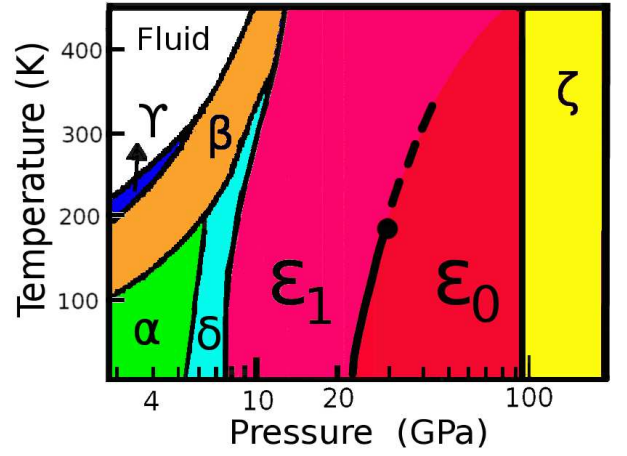


Figure 9: (Color online) Proposed new phase diagram of oxygen.

and very considerably broadened, to the extent that its vibrational satellites are not anymore distinguishable.¹⁵ That optical observation can now be explained.

In the $S = 1$ Heisenberg model representation, the ${}^3\Sigma_g^- \rightarrow {}^1\Delta_g$ excitation of a single molecule amounts to annihilating a spin 1 site in a plaquette leaving a vacancy in its place. We should expect optical absorption at a frequency equal to the $E_{{}^3\Sigma_g^- \rightarrow {}^1\Delta_g}$ molecular excitation energy plus the energy cost of the molecular vacancy. An experimental estimate of this cost was given as a mere 250 cm^{-1} in the δ -phase at much lower pressure¹⁵, where the absorption peak is close to the molecular excitation energy and its broadening, attributable to shake up of spin waves, is small. As pressure rises the exchange coupling J_1 increases rapidly, as signaled by the blue shift and broadening of this transition visible within the δ -phase.¹⁵ In the O₂ quartet singlet state, a vacancy costs roughly the energy difference between the ground state of the three surviving O₂ molecules and the initial four-molecule state. This difference is readily found to be $3J_1$. Moreover, since the three molecule state has $S = 1$, while the initial four molecule state was a singlet, an itinerant spin-1 excitation must be created in addition to the vacancy, costing an additional energy $\omega \in [J_1 - 4J_2, J_1 + 4J_2]$ (see Inset in Fig.8). We therefore predict the absorption line to undergo at the $\delta \rightarrow \epsilon$ transition a sudden blue shift of $\lesssim 4(J_1 - J_2)$ with a large broadening $\sim 8J_2$ due to inter-plaquette exchange. With the calculated exchange values at 11.4 GPa that means $\simeq 0.54 \text{ eV} = 4355 \text{ cm}^{-1}$ and $\simeq 0.28 \text{ eV} = 2258 \text{ cm}^{-1}$ respectively, values that are reasonably close to the experimental ones.¹⁵ (see Fig.8). In conclusion, the abrupt change of optical absorption is explained by the onset of a correlated singlet state at the $\delta \rightarrow \epsilon$ transition.

IV. NEW PHASE DIAGRAM

The ground state of high pressure ϵ -O₂, correctly described as a Peierls-distorted nonmagnetic band insulator and an overall spin singlet above 20 GPa, turns below 20 GPa into a correlated insulator, where molecules recover their S=1 spin, but where exchange couplings and quantum fluctuations between spins conspire to yield another, different overall spin singlet ground state. Sharing very similar quartet lattice structures, the two states appear to have similar symmetry, and the question is whether the phase diagram should show a phase transition between the two or not. Assuming same symmetry, there could only be a first order transition or a smooth crossover. On account of the mechanical coupling which the onset of molecular spin must exert on the overall lattice structure, the likeliest candidate is a first order transition.

As it turns out, there is in literature, ignored so far by most, a rather clear evidence of a low temperature, first order phase transition¹⁷, signaled around 25 GPa at 20 K by a small but sharp and sudden 10 cm⁻¹ splitting of a low frequency vibration. We propose that this could signal precisely the first order line separating the low pressure phase, say ϵ_1 -O₂, and the high pressure one, say ϵ_0 -O₂. This phase line will extend at finite temperature but, on account of same symmetry, should terminate with a critical point. Because there are underlying spins in ϵ_1 -O₂ but not in ϵ_0 -O₂, the phase line must turn towards higher pressures as temperature grows, because ϵ_1 -O₂ possesses a high temperature spin entropy $S \sim \ln 3$ per molecule whereas ϵ_0 -O₂ does not. Accurate room temperature vibrational data¹⁶ actually indicates a *smooth* crossover between unsplit and split modes above 30 GPa, a pressure definitely higher than the 20 K sharp transition near 25 GPa. That confirms our suggestion, and supports the prediction of a critical point below 300 K and near 30 GPa. Our new proposed phase diagram

is therefore summarized in Fig.9.

V. CONCLUSIONS

A fresh ab initio study connects with existing vibrational evidence to indicate that molecular spin plays an important role in the lower pressure part of the ϵ -O₂ oxygen phase diagram. Specifically, we propose replacing the single broad ϵ -O₂ phase from 8 to 96 GPa with two phases ϵ_1 -O₂ and ϵ_0 -O₂ – the first a local singlet spin 1 liquid, the second a regular, Peierls band insulator – separated by a first order phase transition near 20 GPa. The predicted phase line should evolve with temperature, terminating with a novel critical point, probably near 30 GPa and 200 K. The high temperature region below 30 GPa must be characterized by thermally fluctuating S=1 spins, whose presence should be directly detectable by magnetic susceptibility measurements in the 8-30 GPa pressure range. At low temperatures, the wealth of low energy spin excitations present in ϵ_1 -O₂ but absent in ϵ_0 -O₂ should in addition give rise to very new energy dissipation channels and processes in the former phase.

Acknowledgments

The authors would like to thank G. Baskaran, Otto Gonzales, Sadhana Chalise, Carlos Pinilla and Nicola Seriani for fruitful discussions. This work and in particular YC's position was partly sponsored by ERC Advanced Grant 320796 – MODPHYSFRICT. Contracts PRIN/ COFIN 2010LLKJBX 004 and 2010LLKJBX 007, EU-Japan Project LEMSUPER, and Sinergia CR-SII2136287/1 are also acknowledged.

¹ G. Weck and S. Desgreniers and P. Loubeyre and M. Mezouar, *Single-Crystal Structural Characterization of the Metallic Phase of Oxygen*, *Phys. Rev. Lett.* 102 (2009) pp 255503–255506.

² Yu. A. Freiman and H. J. Jodl, *Solid oxygen, Physics. Reports.*, 401, (2004), pp .1-228.

³ L. F. Lundegaard, G. Weck, M. I. McMahon, S. Desgreniers, and P. Loubeyre, *Observation of an O₈ molecular lattice in the [ε] phase of solid oxygen*, *Nature*, 443, (2006), pp. 201–204.

⁴ H. Fujihisa, *et al.* O₈ Cluster Structure of the Epsilon Phase of Solid Oxygen, *Phys. Rev. Lett.*, 97, (2006), pp. 085503–085506.

⁵ I. N. Goncharenko, *Evidence for a Magnetic Collapse in the Epsilon Phase of Solid Oxygen*, *Phys. Rev. Lett.*, 94, (2005), pp. 205701–205704.

⁶ S. Serra, G. Chiarotti, S. Scandolo, and E. Tosatti, *Pressure-Induced Magnetic Collapse and Metallization of Molecular Oxygen: The ζ-O₂ Phase*, *Phys. Rev. Lett.*, 80,

(1998), pp. 5160–5163.

⁷ F. A. Gorelli, L. Ulivi, M. Santoro, and R. Bini, *The ε Phase of Solid Oxygen: Evidence of an O₄ Molecule Lattice*, *Phys. Rev. Lett.*, 83, (1999), pp. 4093–4096.

⁸ J. B. Neaton, and N. W. Ashcroft, *Low-Energy Linear Structures in Dense Oxygen: Implications for the ε Phase*, *Phys. Rev. Lett.*, 88, (2002), pp. 205503–205506.

⁹ B. Militzer, and R. J. Hemley, *Crystallography: Solid oxygen takes shape*, *Nature*, 443, (2006), pp. 150–151.

¹⁰ Ma. Yanming, A. R. Oganov, and C. W. Glass, *Structure of the metallic ζ-phase of oxygen and isosymmetric nature of the ε-ζ phase transition: Ab initio simulations*, *Phys. Rev. B*, 76, (2007), pp. 064101–064105

¹¹ T. Anh Pham, R. Gebauer, and S. Scandolo, *Magnetism and vibrations in the phase of oxygen*, *Solid State Communications*, 149, (2009), pp. 160 – 162.

¹² H. V. Gomonay and V. M. Loktev, *Magnetoelastic nature of the solid oxygen ε-phase structure*, *Phys. Rev. B*, 76, (2007), pp. 094423–094431.

- ¹³ , M. Bartolomei, et al. *Molecular oxygen tetramer (O₂)₄: Intermolecular interactions and implications for the ϵ solid phase*, *Phys. Rev. B*, 84, (2011), pp. 092105–092108.
- ¹⁴ F. A. Gorelli, M. Santoro, L. Ulivi, and R. Bini, *Intermolecular interactions in the ϵ phase of solid oxygen studied by infrared spectroscopy*, *Physica B: Condensed Matter*, 265, (1999), pp. 49–53.
- ¹⁵ M. Santoro, F. A. Gorelli, L. Ulivi, R. Bini, and H. J. Jodl, *Antiferromagnetism in the high-pressure phases of solid oxygen: Low-energy electronic transitions*, *Phys. Rev. B*, 64 (2001), pp. 064428–064434.
- ¹⁶ Y. Akahama and H. Kawamura, *High-pressure Raman spectroscopy of solid oxygen*, *Phys. Rev. B*, 54, (1996), pp. R15602–R15605.
- ¹⁷ W. B. Carter, D. Schiferl, M. L. Lowe and D. Gonzales, *New phase of oxygen at high pressure and low temperature*, *The Journal of Physical Chemistry*, 95, (1991), pp. 2516–2519.
- ¹⁸ L. Ulivi, (2002) Quantitative spectroscopy of simple molecular crystals under pressure. *High pressure phenomena: Proceedings of the International School of Physics "Enrico Fermi"*, eds R. J. Hemley, G. L. Chiarotti, M. Bernasconi, L. Ulivi (IOS Press, Amsterdam) pp.-337
- ¹⁹ V. I. Anisimov, J. Zaanen, and O. K. Andersen, *Band theory and Mott insulators: Hubbard U instead of Stoner I* , *Phys. Rev. B*, 44, (1991), pp. 943–954.
- ²⁰ V. I. Anisimov, I. V. Solovyev, M. A. Korotin, M. T. Czyżyk, and G. A. Sawatzky, *Density-functional theory and NiO photoemission spectra*, *Phys. Rev. B*, 48, (1993), pp. 16929–16934.
- ²¹ A. I. Liechtenstein, V. I. Anisimov, and J. Zaanen, *Density-functional theory and strong interactions: Orbital ordering in Mott-Hubbard insulators*, *Phys. Rev. B*, 52, (1995), pp. R5467–R5470.
- ²² P. Giannozzi, et al., *QUANTUM ESPRESSO: a modular and open-source software project for quantum simulations of materials*, *Journal of Physics: Condensed Matter*, 21, (2009), pp. 395502
- ²³ J. P. Perdew, K. Burke, and M. Ernzerhof, *Generalized Gradient Approximation Made Simple*, *Phys. Rev. Lett.*, 77, (1996), pp. 3865–3868.
- ²⁴ S. L. Dudarev, G. A. Botton, S. Y. Savrasov, C. J. Humphreys, and A. P. Sutton, *Electron-energy-loss spectra and the structural stability of nickel oxide: An LSDA+ U study*, *Phys. Rev. B*, 57, (1998), pp. 1505–1509.
- ²⁵ , M. Cococcioni, and S. de Gironcoli, *Linear response approach to the calculation of the effective interaction parameters in the LDA + U method*, *Phys. Rev. B*, 71, (2005), pp. 035105–035121.
- ²⁶ H. J. Monkhorst, and J. D. Pack, *Special points for Brillouin-zone integrations*, *Phys. Rev. B*, 13, (1976), pp. 5188–5192.
- ²⁷ A. Togo, F. Oba and I. Tanaka, *First-principles calculations of the ferroelastic transition between rutile-type and CaCl₂-type SiO₂ at high pressures*, *Phys. Rev. B*, 78, (2008), pp. 134106–134114.
- ²⁸ S. Baroni, S. de Gironcoli, A. Dal Corso, and P. Giannozzi, *Phonons and related crystal properties from density-functional perturbation theory*, *Rev. Mod. Phys.*, 73, (2001), pp. 515–562.
- ²⁹ G. Herzberg (1996) *Molecular spectra and molecular structure, v.3: Electronic spectra and electronic structure of polyatomic molecules*. eds (Princeton, NJ : Van Nostrand)